International Journal of Electrochemical Science 19 (2024) 100715

Contents lists available at ScienceDirect

International Journal of Electrochemical Science

journal homepage: www.editorialmanager.com/ijoes

Enhancing the performance of pyridyl carboxamide-N,N-dimethyl amino chalcone (PCC) as a dye sensitizer for dye-sensitized solar cells (DSSCs) through the incorporation of electron donor moieties

Maadh F. Nassar [a,b,*], Emilia Abdulmalek [a,b,*], Mohd F. Ismail [b], Shahrul Ainliah Alang Ahmad [b]

[a] Integrated Chemical Biophysics Research, Faculty of Science, Universiti Putra Malaysia, Serdang, Selangor 43400 UPM, Malaysia
[b] Department of Chemistry, Faculty of Science, Universiti Putra Malaysia, Serdang, Selangor 43400 UPM, Malaysia

ARTICLE INFO

Keywords:
PCC
Dye-sensitized solar cells
DSSCs
DFT
TD-DFT

ABSTRACT

This study has focused on enhancing the performance of pyridyl carboxamide-N,N-dimethyl amino chalcone (PCC) as a sensitizer for dye-sensitized solar cells (DSSCs) by strategically incorporating electron donor moieties identified in a literature review. Our reviewing the previous reports highlights the pivotal role of electron donors in optimizing light harvesting, electron injection, and overall power conversion efficiency in organic dye sensitizers, particularly those following a donor-bridge-acceptor (D-π-A) architecture. The selected donor moieties, including dithieno[3,2-b:2′,3′-d]thiophene (DTT), benzodithiophene (BDT), triphenylamine (TPA), carbazole (CBZ), and triazatruxene (TAZ), are systematically introduced into the molecular structure of PCC (abbreviated as PCC-DTT, PCC-BDT, PCC-TPA, PCC-CBZ, and PCC-TAZ, respectively). The performance of these modified compounds is rigorously evaluated using density functional theory (DFT) methods. Validation results revealed that the most reliable method for PCC derivative characterization involved the combination of the functional B3PW91 with a 6-31G(d) basis set. The results indicate that the incorporation of certain donor moieties, particularly BDT, significantly enhances the electronic and optical properties of PCC, including lower HOMO energy levels, a narrow energy gap (E_{gap}), enhanced absorption intensity, and a redshift in absorption peaks. Evaluation of photovoltaic properties including electron injection (ΔG_{inj}), and open circuit voltage (V_{oc}), indicated facilitating spontaneous electron injection from the dyes to the TiO_2 conduction band. Notably, PCC-TAZ demonstrated the lowest electron regeneration (ΔG_{reg}), suggesting a notable potential for efficient electron regeneration.

1. Introduction

As the need for clean and renewable energy technologies has grown in the last several years, much research has been done to find materials with remarkable optoelectronic characteristics [1,2]. These materials are receiving more attention because of their many benefits, which include minimal propagation loss, high output, outstanding compatibility, affordability, high stability, and low toxicity [3–5]. As a result, these materials have been widely used in a variety of technological fields, including laser diodes [6], passive and active remote sensing [7], thin-film-transistors (TFTs) [8], optoelectronic devices [9], and solar cells [10]. The development of dye-sensitized solar cells (DSSCs) has drawn growing interest, notably due to an increase in research efforts aimed at achieving high power conversion efficiency (PCE) and easy manufacturing of optoelectronic materials. Metal-based complex dyes and metal-free organic dyes are the two main classes of DSSCs [11]. Metal-based complex dyes typically involve the incorporation of transition metal complexes, such as ruthenium [12] and osmium [13], as the central photoactive components. These metal complexes play a crucial role in efficiently absorbing sunlight and facilitating charge separation within the cell. The choice of metal and ligands in these complexes significantly influences the absorption spectra and redox properties, thereby impacting the overall performance of the DSSC [14]. On the other hand, metal-free organic dyes utilize organic molecules as sensitizers, often composed of conjugated π-systems [15,16]. These organic dyes, owing to their tunable chemical structures, offer versatility in design and synthesis. The absorption characteristics of metal-free organic dyes are influenced by the extent of conjugation and

* Corresponding authors at: Integrated Chemical Biophysics Research, Faculty of Science, Universiti Putra Malaysia, Serdang, Selangor 43400 UPM, Malaysia.
E-mail addresses: nassarmaadh@gmail.com (M.F. Nassar), emilia@upm.edu.my (E. Abdulmalek).

https://doi.org/10.1016/j.ijoes.2024.100715
Received 28 May 2024; Received in revised form 25 June 2024; Accepted 5 July 2024
Available online 6 July 2024

functional groups, enabling customization for optimal light absorption in the visible spectrum [17]. The absence of heavy metal atoms simplifies the electron injection process from the excited dye into the semiconductor, facilitating efficient charge separation within the DSSC. This improved charge transport contributes to higher overall device performance [18]. Additionally, metal-free organic dyes tend to exhibit better stability and resistance to degradation under prolonged exposure to light and harsh environmental conditions. This increased stability enhances the durability and longevity of DSSCs, making them more practical for real-world applications [19].

The maximum improvement in organic dye sensitizer efficiency is attained by adding a sophisticated donor-bridge-acceptor (D-π-A) design. A π-conjugated bridge that makes opposing connections with both electron donor (D) and electron acceptor (A) groups is a feature of this architectural framework [20–22]. The strategic design of this π-conjugated bridge emerges as a pivotal element in tailoring the energy levels of D-π-A organic dye sensitizers. This meticulous design approach not only enhances the overall performance of the organic dye sensitizers but also underscores the importance of rational molecular engineering in advancing the field of dye-sensitized solar cells [23,24]. So far, many studies have introduced promising D moieties for the dye D-π-A architecture. For example, Lin et al. [25] explored the use of the electron donor dithieno[3,2-b:2′,3′-*d*]thiophene (DTT) as a unique moiety for sensitizers. Using oligothiophene as a spacer, 2-cyanoacrylic acid as an acceptor, and DTT as a donor group, the authors created several compounds. Using the ruthenium dye N719, the study notably shed light on the performance of DSSCs made using these DTT-based sensitizers, which achieved efficiencies of almost 70 % in comparison to the conventional cell. The outcomes demonstrated the importance of electron-donating moieties, like DTT, in the development of organic sensitizers free of metals for improved solar cell efficiency. In another study, novel star-shaped small-molecule donors, BDT-3Th and BDT-4Th, were designed for use in organic solar cells (OSCs) [26]. The emphasis was on the D group, particularly the benzodithiophene (BDT) unit known for its large planar conjugated structure. The experimental results demonstrated that the four-armed BDT-4Th exhibited a relatively blue-shifted absorption spectrum, higher extinction coefficient, deeper HOMO energy level, and improved phase separation morphology when blended with Y6, a non-fullerene acceptor. The performance of the BDT-4Th:Y6-based OSC device achieved a significant enhancement with a power conversion efficiency (PCE) of 5.83 %, surpassing the efficiency of the BDT-3Th:Y6-based device (PCE = 3.78 %). The increased PCE was attributed to higher short-circuit current density (J_{sc}) and fill factor (FF) in the BDT-4Th:Y6 system, indicating the importance of the BDT-based electron-donor unit in achieving improved photovoltaic properties. Liang Han and colleagues [27] synthesized three D-D-π-A triphenylamine-coumarin sensitizers with different π-bridges (thiophene, bithiophene, and phenylthiophene) and investigated their photoelectric conversion efficiency. The privilege of utilizing triphenylamine was previously suggested by Jia et al. [28]. They found that the introduction of phenothiazine dye with an additional dithiafulvenyl unit as a donor resulted in increased electron-donating ability and improved power conversion efficiencies from 4.16 % to 5.87 %. In the literature [29], the authors believed that the D group was a critical component in the DSSC process. They presented novel carbazole derivatives as sensitizers for DSSC, aiming to understand their donation capacity. DFT and time-dependent DFT calculations indicated significant intramolecular charge transfer occurring from the highest occupied molecular orbital (HOMO) to the lowest unoccupied molecular orbital (LUMO), despite the donor carbazole being twisted (~ 51°) concerning the conjugated spacer. The study suggested that tuning carbazole derivatives can enhance their role as sensitizers in DSSC. Two novel dye sensitizers named JY04 and JY05 were prepared based on triazatruxene as the electron donor and rhodanine-3-acetic acid as the electron acceptor [30]. According to a photovoltaic performance investigation, JY05 outperformed JY04 in terms of light harvesting, electron injection efficiency, and power conversion efficiency when using a benzene conjugation as the π-conjugated linker. The review of the studies mentioned above collectively points to the critical contribution of electron donors in enhancing the performance of sensitizers in DSSCs, emphasizing their role in achieving improved light harvesting, electron injection, and overall power conversion efficiency.

Pyridyl carboxamide-N,N-dimethyl amino chalcone (PCC) is a novel organic compound synthesized for studying its linear and nonlinear optical (NLO) characteristics [31,32]. The compound is designed based on the molecular structure of chalcone derivatives, known for their favorable NLO responses. Specifically, the incorporation of a pyridyl carboxamide group and N,N-dimethyl amino moiety in the chalcone framework characterizes PCC. The choice of N,N-dimethyl amino chalcone is motivated by previous findings that chalcone derivatives, especially those containing N,N-dimethyl units, exhibited good optical properties and promising sensitizers for DSSCs. A sophisticated D-π-A architecture of PCC allows precise manipulation of the absorption spectra and electronic properties of the dye, optimizing its light-harvesting capabilities. Notable examples include studies using electron donors such as dithieno[3,2-b:2′,3′-*d*]thiophene (DTT), benzodithiophene (BDT), triphenylamine (TPA), carbazole (CBZ), and triazatruxene (TAZ). However, the synthesized pyridyl carboxamide-N,N-dimethyl amino chalcone (PCC) lacks any electron donor group, which raises a significant concern regarding its potential as a sensitizer for DSSCs. In the context of the well-established importance of electron donors, the absence of such a group in PCC prompts the question of whether it can effectively contribute to the enhancement of NLO responses, as demonstrated in studies with electron-rich donors.

The primary goal of this work is to improve the performance of PCC (used as a sensitizer) in DSSCs. The improvement will be achieved by incorporating specific electron donor groups into the PCC molecule. Previous studies have extensively reviewed the role of electron donor groups, emphasizing their importance in achieving optimal light absorption, efficient electron injection, and overall power conversion efficiency in organic dye sensitizers, particularly those following a D-π-A architecture. We plan to strategically introduce electron donor moieties into PCC. These moieties include Dithieno[3,2-b:2′,3′-d]thiophene (DTT), Benzodithiophene (BDT), Triphenylamine (TPA), Carbazole (CBZ), and Triazatruxene (TAZ). Each modified compound will be labeled as PCC-DTT, PCC-BDT, PCC-TPA, PCC-CBZ, and PCC-TAZ (Fig. 1). To evaluate the performance of these modified compounds, we will use theoretical calculations based on the density functional theory (DFT) method. DFT calculations provide insights into the geometrical, electronic, and optical properties of the modified sensitizers, aiding in the prediction and optimization of their photovoltaic properties.

2. Computational details

Using density functional theory (DFT) and time-dependent DFT (TD-DFT) techniques, the five PCC derivatives were thoroughly examined. The Gaussian 09 software package carried out all of the computations [33,34]. Finding each compound's ground state in dimethyl sulfoxide (DMSO) under experimentally-like conditions was our primary goal [31]. The integral equation formalism model of the polarizable continuum model (IEFPCM) [35] was used to describe the solvent. The geometry optimization, crucial for understanding molecular structures, was carried out through a hybrid DFT level of computation, specifically employing the B3PW91 (Perdew and Wang correlation) exchanged-correlation function and a 6–31 G(d) basis set [36,37]. The Supplementary information (SI.1) contains comprehensive coordinates for all optimized structures. To ensure that these structures accurately corresponded to local minima on the potential energy surface, frequency calculations were conducted using the same level of computation, and the results indicated an imaginary frequency of zero (NImag = 0) [38,39].

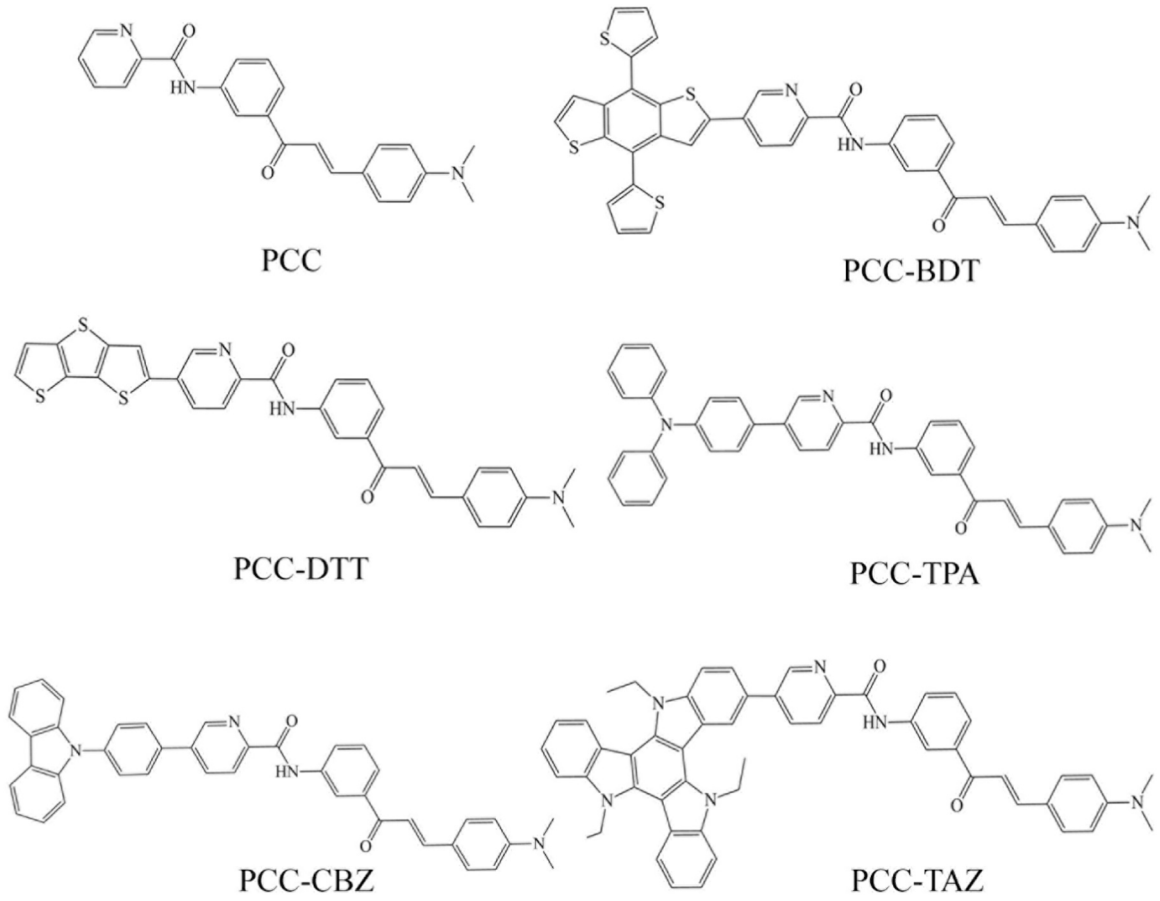

Fig. 1. Two-dimensional structure of PCC and its derivatives.

The structural parameters and electronic properties, in particular the frontier molecular orbitals (FMOs) of the successfully optimized structures, were evaluated to conduct a more thorough examination. Next, the TD-DFT technique became essential to estimate the optical adsorption. Using 6-31G(d) basis sets, five optimization and UV-Vis adsorption calculation methods were used: B3LYP, B3PW91, BVP86, CAM-B3LYP, and PBEPBE. Considering the reference compound PCC and adhering to the solvent effect, DMSO was applied via the IEFPCM model. The calculated wavelengths of maximum absorption (λ_{max}) using B3LYP/6-31G(d), B3PW91/6-31G(d), BVP86/6-31G(d), CAM-B3LYP/6-31G(d), and PBEPBE/6-31G(d) outputs were 427.5, 427.1, 571.0, 358.2, and 570.3 nm, respectively. Notably, the comparison with the experimental value of 424 nm for PCC in DMSO [31] established that B3LYP and B3PW91 were among the most reliable DFT functions. Despite this, we were interested in pursuing our investigation using the B3PW91/6-31G(d) method as it was relatively closer to the experimental record. After achieving satisfactory validation with experimental value through TD-DFT/B3PW91/6-31G(d), all the PCC derivatives in this study were consistently calculated using the same level and basis set. Our comprehensive analysis delved into four key aspects: structural, electronic, optical, and photovoltaic properties, providing a holistic understanding of the compounds under scrutiny [40–42].

3. Results and discussion

3.1. Structural properties

Organic dyes play a pivotal role as sensitizers in DSSCs, absorbing sunlight and facilitating the generation of photo-excited electrons. Understanding the structural characteristics of these compounds is imperative for optimizing their electron injections [43,44]. Electron-donating groups can lead to shorter bond lengths between atoms. This effect occurs because the additional electron density from the donor group strengthens the bond. Larger bond angles often result in shorter bond lengths. When bond angles increase, the repulsion between adjacent atoms decreases, allowing them to come closer together. Therefore, it should be noted that incorporating electron donor moieties can alter bond lengths and angles, impacting the overall geometry of the molecule [45,46]. DFT calculations can generate highly accurate estimations of structural parameters. DFT calculations also assist in unraveling the intricate relationships between the molecular structure of dye compounds and their electronic and optical properties, as well as their photovoltaic performance [47–49]. Fig. 2 illustrates the area in PCC

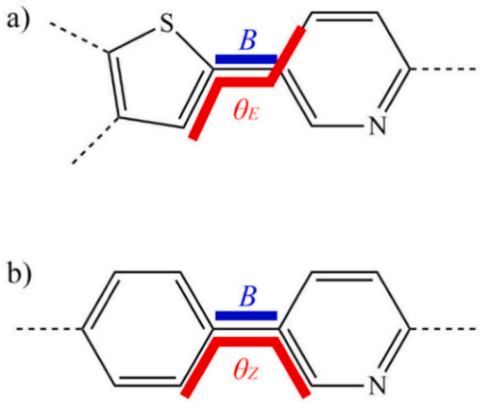

Fig. 2. The position of B, θ_E, and θ_Z in a) PCC-DTT and PCC-BDT and b) PCC-TPA, PCC-CBZ and PCC-TAZ.

derivatives where a donor group (D) is connected with a π-conjugated unit. The bond distance is represented by *B*, and the dihedral angles are denoted as θ_E and θ_Z, describing the relative orientations of the donor (D) and π-conjugated unit. The dihedral angles affect the overlap of molecular orbitals, impacting electronic coupling. All the values of bond distances and dihedral angles are listed in Table 1. The value of *B* showed an increased trend as the order of PCC-DTT < PCC-BDT < PCC-TPA < PCC-TAZ < PCC-CBZ. It was found that when the D group expanded in size, the bond distance (*B*) lengthened. The small *B* value in PCC-DTT and PCC-BDT indicated a stronger connection between the D group and the π-conjugated unit. This observation could be attributed to electron-rich thiophene rings in DTT and BDT structure which strongly transferred electrons to the π-conjugated unit. We could describe the relative orientations of adjacent molecular planes by evaluating the dihedral angles. The values of θ_E for PCC-DTT and PCC-BDT were much closer to 180 degrees and the values of θ_Z were much closer to 0 degrees. The values of dihedral angles showed that the combination of DTT and BDT groups with PCC made the most planar formation in the connecting area between the donor (D) and π-conjugated units. However, PCC-TAZ recorded a θ_E value of 142.148° and a θ_Z value of − 38.443°, indicating the least flat connecting area between the TAZ group and the PCC molecule. Being a planar connecting area among each component D, π-spacer, and A is crucial since it leads to stronger molecular orbital overlapping, electronic interactions, and charge transfers [50–52]. Therefore, to gain a deeper comprehension of electronic aspects, including molecular orbitals and charge transfers, it is necessary to examine the electronic properties of the PCC derivatives.

3.2. Electronic properties

DFT calculations provide valuable insights into the energy levels, molecular orbitals, and charge distribution within organic dyes. Understanding the electronic structure aids in predicting absorption spectra, charge transfer processes, and overall device efficiency [53,54]. These properties can be computationally explored through two analyses: i) frontier molecular orbital (FMO) and ii) molecular electrostatic potential (MEP) surface [55–57]. The highest occupied molecular orbital (HOMO) and the lowest unoccupied molecular orbital (LUMO) are two essential orbitals that are the focus of the FMO theory. The energy gap between the HOMO and LUMO orbitals, known as the E_{gap}, is indicative of the molecule's reactivity and stability. Fig. 3 presents the values of the energy level of HOMO (E_{HOMO}), LUMO (E_{LUMO}), and E_{gap} for the five PCC derivatives calculated using the B3PW91/6-31G(d) method. Significantly, the HOMO energy (E_{HOMO}) levels of the compounds consistently remained below the energy level of the electrolyte I^-/I^{-3} (-4.80 eV). This suggests the possibility of regenerating the oxidized dye by gaining an electron from the electrolyte. Additionally, the LUMO energy (E_{LUMO}) levels of the compounds were observed to be higher than the conduction band of TiO_2 (-4.0 eV), promoting efficient electron transport from the excited dye to the semiconductor. The E_{HOMO} values range from − 5.19 to − 5.33 eV, whereas the E_{LUMO} values range from − 2.16 to − 2.37 eV. A lower energy level of the HOMO is generally associated with easier electron donation. Thus, from the data, PCC-DTT, PCC-BDT, and PCC-CBZ had relatively lower E_{HOMO} and potential for electron donation. Among all E_{gap} values ranging from 2.96 to 3.16 eV,

Table 1
The values of *B*, θ_E, and θ_Z of PCC derivatives calculated by B3PW91/6-31G(d) method.

Compounds	*B*	θ_E	θ_Z
PCC-DTT	1.457	-156.670	23.588
PCC-BDT	1.460	-156.095	24.168
PCC-TPA	1.473	146.353	-34.090
PCC-CBZ	1.477	143.992	-36.389
PCC-TAZ	1.476	142.148	-38.443

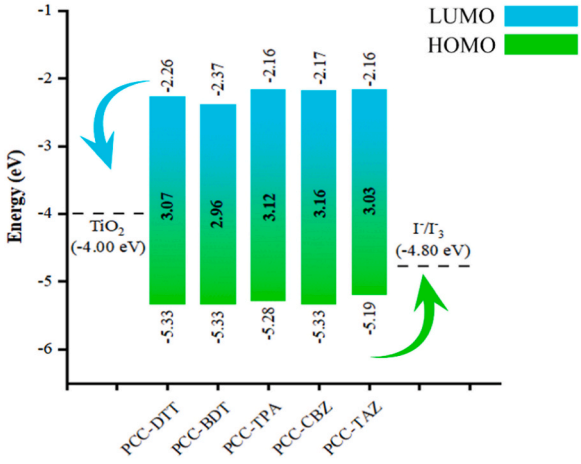

Fig. 3. Energy level diagram of PCC derivatives calculated by B3PW91/6-31G (d) method.

PCC-BDT experienced the lowest value indicating a lower energy barrier for electron transitions. The narrowest E_{gap} in PCC-BDT also implies that the dye can absorb photons with lower energy. So far, it is believed that the combination of PCC with BDT (as a donor group) made an excellent promising conjugated D-π-system for future organic dye.

In general, the HOMO is supposed to be localized on the donor moiety, reflecting its electron-donating nature, while the LUMO is supposed to be delocalized over the acceptor, signifying its electron-accepting property. The π-conjugated bridge plays a pivotal role in mediating electronic communication between the donor and acceptor, influencing the overall efficiency of the dye sensitizers in converting solar energy. Fig. 4 shows the HOMO and LUMO distribution patterns as well as MEP maps for the PCC derivatives in their ground state. Accordingly, PCC-DTT, PCC-BDT, PCC-TPA, and PCC-TAZ were among the most desirable samples. Because HOMO orbitals were concentrated on different types of donor groups, whereas LUMO orbitals were concentrated on the PCC molecules' terminals. Therefore, it can be said that these derivatives were capable of successful charge transfer from the suggested group to the π-spacer, PCC. However, PCC-CBZ did not display a favorable case since both HOMO and LUMO orbitals were distributed on the PCC molecule. The MEP relies on a range between negative and positive values for each case, which is mentioned in the bracket; PCC-DTT (-0.0756e to 0.0756e), PCC-BDT (-0.0758e to 0.0758e), PCC-TPA (-0.0775e to 0.0775e), PCC-CBZ (-0.0748e to 0.0748e), PCC-TAZ (-0.0753e to 0.0753e). Based on the results observed from the MEP maps, the carbonyl group of PCC had the highest electron density area (red color). In contrast, the PCC molecules' terminals illustrated the lowest electron density area (light blue color). Also, some yellow spots on the donor groups and over the PCC structure imply the electron transfer from donor groups to the π-spacer, PCC. Although the overall shape and distribution of potentials in the MEP maps are consistent, their subtle distinctions can significantly affect molecular behavior. Evaluating the dipole moments in this study is indeed important because dipole moments play a crucial role in charge transfer processes. The dipole moment in three dimensions (x, y, and z) represents the separation of positive and negative charges within a molecule. Besides the total value of dipole moments displayed in Fig. 4, the values of dipole moments in three dimensions are available in Table SI.1. The greatest value of dipole moment belongs to PCC-CBZ (7.30 Debye), and the majority of this value is taken from the contribution of the x-axis (-6.80 Debye). The blue arrows in Fig. 4 confirm that the dipole moment in PCC-CBZ is mainly directed towards the x-axis. Besides analyzing HOMO and LUMO orbitals, MEP maps, and dipole moment, it is also required to examine the optical properties of the PCC derivatives for further confirmation.

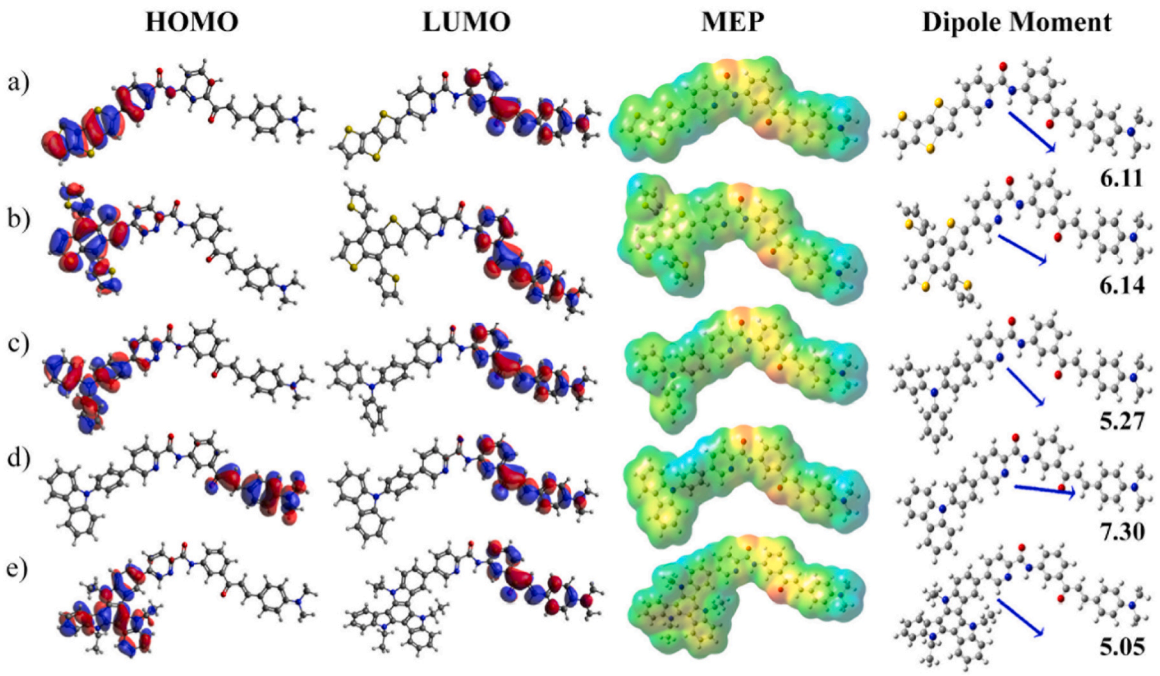

Fig. 4. FMOs, MEP and dipole moment for a) PCC-DTT, b) PCC-BDT, c) PCC-TPA, d) PCC-CBZ and e) PCC-TAZ.

3.3. Optical properties

Optical property analysis complements the study of the electronic properties of the PCC derivatives, providing a comprehensive understanding of their behavior in response to light. An extensive computational investigation was carried out on each PCC derivative utilizing the B3PW91/6-31G(d) method to thoroughly evaluate the optical characteristics within a DMSO solution. The objective of this methodology was to clarify the role of molecular orbitals in electronic transmissions, resulting in the derivation of essential parameters including maximum absorption (λ_{max}), excitation energies (E_{ex}), oscillator strength (*f*), and major contribution. This analytical approach aimed to provide a detailed understanding of the dye's optical behavior, offering insights into electronic transitions and key parameters. Table 2 details the parameters mentioned above (its full data is provided in Section SI.3), and Fig. 5 depicts a comparative simulated absorption spectra of PCC derivatives in DMSO. The strongest adsorption peaks were extracted from

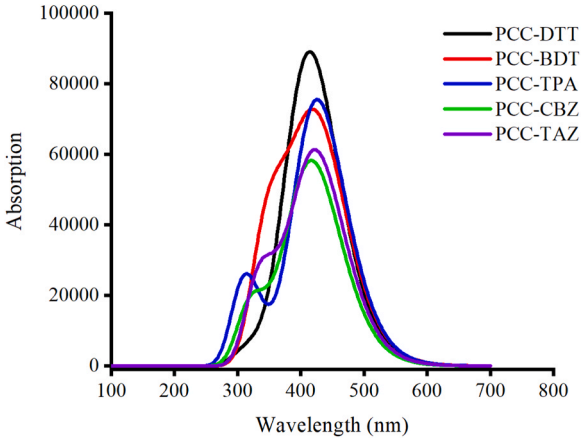

Fig. 5. Comparative absorption spectra of title compounds.

Table 2
The calculated values of optical parameters for PCC derivatives calculated by the B3PW91/6-31G(d) method.

Compounds	E_{ex} (eV)	λ (nm)	*f*	Major contribution
PCC-DTT	2.85	435.5	0.009	H → L (71 %)
	2.92	425.3	1.491	H → L + 1 (68 %), H-1 → L (15 %)
	3.141	394.7	0.856	H-1 → L (68 %), H → L + 1 (15 %)
PCC-BDT	2.75	451.7	0.005	H → L (71 %)
	2.85	435.7	0.577	H-1 → L (67 %), H → L + 1 (20 %)
	2.93	423.7	1.069	H → L + 1 (67 %), H-1 → L (20 %)
PCC-TPA	2.89	428.3	1.124	H → L (36 %), H → L + 1 (43 %), H-1 → L (42 %)
	2.91	426.4	0.522	H → L (59 %), H-1 → L (36 %), H → L+1 (13 %)
	2.97	417.6	0.193	H → L + 1 (54 %), H-1 → L (43 %), H → L (15 %)
PCC-CBZ	2.92	424.9	1.146	H → L (70 %)
	3.05	406.3	0.104	H → L + 1 (70 %)
	3.22	384.9	0.299	H-1 → L + 1 (66 %), H-1 → L (24 %)
PCC-TAZ	2.83	438.5	1.267	H → L (70 %)
	2.88	430.9	0.007	H-1 → L (70 %)
	2.91	425.9	0.001	H-2 → L (61 %), H → L + 1 (34 %)

the first major promotion of the HOMO to LUMO, as detailed in the preceding section (see Fig. 4). Additionally, the transition from HOMO-1 to LUMO and HOMO to LUMO+1 was observed as the second common major promotion. All the molecular orbitals related to Table 2 (such as HOMO, LUMO, H-1, and L + 1) are available in section SI.4. The compound PCC-BDT exhibited the lowest excitation energy (E_{ex} = 2.75 eV) and the longest absorption wavelength (λ = 451.7 nm), indicating a noticeable red shift. In contrast, PCC-CBZ displayed the highest value of excitation energy (E_{ex} = 2.92 eV) and an absorption wavelength of 424.9 nm. Besides that, PCC-DTT, PCC-TPA, and PCC-TAZ showed quite similar values of E_{ex} and λ_{max}. PCC-CBZ exhibited a distinct HOMO compared to other molecules (PCC-DTT, PCC-BDT, PCC-TPA, and PCC-TAZ). Electron delocalization within the molecule might impact the energy levels of HOMO and LUMO in PCC-CBZ [58,59]. On the other side, PCC-CBZ (green curve) exhibited a unique absorption pattern compared to the other compounds. Its peak absorption wavelength differs from the rest, indicating distinct electronic transitions. Therefore, the unique HOMO distribution in PCC-CBZ likely influences its absorption behavior. It is believed that the interplay between molecular

structure, donor moieties, and electronic transitions explains why PCC-CBZ stands out in its UV–visible absorption spectrum.

All the simulated UV–Vis absorption spectra revealed a significant enhancement in absorption intensity with the development of the suggested D moieties, except for PCC-CBZ. As described in the previous section, our theoretical method, B3PW91/6-31G(d), was validated with an experimental value of λ_{max} for PCC (424 nm) [31]. According to Table 2 and Fig. 5, incorporating DTT, BDT, TPA, and TAZ groups on the PCC structure caused an increase of λ_{max} value to 435.5, 451.7, 428.3, and 438.5 nm, respectively. PCC-BDT not only produced the greatest λ_{max} value but also created the broadest UV–Vis absorption (red peak). It can be said that the expanded π-conjugated D group containing sulfur had a positive impact influencing the broadening, shift, and strength of the absorption peaks [60–62]. Consequently, the incorporation of BDT moiety on PCC contributed to a further broadening of the UV–Vis absorption peaks. All in all, the PCC-based dyes incorporated by the donor group which was greater π-conjugated and contained sulfur showed significant optical properties.

3.4. Photovoltaic properties

This section employs various parameters to assess the photovoltaic properties of the selected dyes. The short-circuit current density (J_{sc}), a key indicator of photovoltaic performance, is influenced by the light-harvesting ability (LHE) and the electron injection free energy (ΔG_{inj}). The mathematical representation of J_{sc} is given by Eq. (1) [63]:

$$J_{sc} = \int_{\lambda} \mathrm{LHE}(\lambda)\Phi_{inj}\eta_{col}\mathrm{d}\lambda \quad (1)$$

here, LHE(λ) is the light-harvesting efficiency, Φ_{inj} indicates the electron injection efficiency, and η_{col} represents the charge collection efficiency. Assuming a constant charge collection efficiency (η_{col}) for DSSCs employing different dyes, the theoretical evaluation of J_{sc} involves obtaining LHE(λ), Φ_{inj}, and total reorganization energy (λ_{total}). LHE is determined using Eq. (2) [64,65]:

$$\mathrm{LHE} = 1 - 10^{-f} \quad (2)$$

where f is the oscillator strength associated with the wavelength of maximum absorption (λ_{max}). In DSSCs, an efficient sensitizer should have a high J_{sc}, which results from a substantial LHE and a high oscillator strength (*f*). Similar to that, Eq. (1) shows that a larger electron injection efficiency (Φ_{inj}), which is related to the driving force of electron injection (ΔG_{inj}), directly correlates with a stronger short-circuit current density (J_{cs}). Eq. (3) is utilized to calculate the latter [66]:

$$\Delta G_{inj} = E_{OX}^{dye*} - E_{CB} \quad (3)$$

where E_{OX}^{dye*} is the excited state oxidation potential energy of the dye concerning the conduction band (CB) of TiO_2, and $E_{CB}^{TiO_2}$ is the reduction potential of the CB of TiO_2. The constants are $E_{CB} = -4.00$ eV, while E_{OX}^{dye*} is determined using Eq. (4) [67]:

$$E_{OX}^{dye*} = E_{OX}^{dye} - E_{ex} \quad (4)$$

In the ground state of dyes, the oxidation potential energy is represented by E_{OX}^{dye} in the Eq. (4), whereas the electronic transition energy that corresponds to λ_{max} is denoted by E_{ex}. Furthermore, Eq. (5) [68,69] is utilized to calculate the driving force of electron regeneration (ΔG_{reg}), which is an essential component for the efficiency of DSSCs.

$$\Delta G_{reg} = E_{OX}^{dye} - E_{redox} \quad (5)$$

Here, E_{redox} represents the redox liquid electrolyte's potential energy, which is − 4.80 eV. Lastly, Eq. (6) calculates the open circuit voltage (V_{oc}) [70,71], or the external maximum voltage output, by measuring the energy difference between the dyes' LUMO orbitals (E_{LUMO}) and the TiO_2 conduction band:

$$V_{oc} = E_{LUMO} - E_{CB} \quad (6)$$

Table 3 compiles the corresponding computed values that were obtained by applying the given equations. The excited state of all PCC derivatives was located above TiO_2's conduction band (CB), as shown by their negative electron injection (ΔG_{inj}) values. As a result, these derivatives spontaneously inject electrons into the conduction band of TiO_2, which transports electrons from the excited states of the dyes. The PCC-TAZ, PCC-TPA, PCC-CBZ, and D groups containing nitrogen were among the most promising choices. Additionally, all ΔG_{reg} values were obtained either equal or lower than the parent compound (PCC = 0.53 eV), signifying that the newly suggested compounds maintained sufficient potential to achieve a high-power conversion efficiency (PCE) for dye-sensitized solar cells (DSSCs). With the lowest ΔG_{reg} value of 0.39 eV, PCC-TAZ was the most efficient example for this purpose. High J_{sc} was a result of a significant value of LHE, which eventually increased the efficiency of DSSCs. In contrast to the value of 0.9164 λ in PCC, the LHE values for all derivatives spanned a broad range, from 0.0124 to 0.9459 λ. These results showed that adding nitrogen-containing D groups to the structures of the new derivative increased the *f* value, which in turn encouraged LHE. All PCC derivatives had V_{oc} values between 1.63 and 1.84 V, with the maximum difference being just 0.21 V between any two dyes. Such slight discrepancies may not significantly impact overall performance, however, understanding the impact of the type of donor moieties on V_{oc} values is crucial for designing solar cells. All of the derivatives' positive V_{oc} values indicated that it was anticipated that electrons from the PCC-based dyes would move easily to the TiO_2 CB. The PCC derivatives containing nitrogen such as PCC-TPA, PCC-CBZ, and PCC-TAZ exhibited a relatively higher V_{oc} value than PCC, whereas the ones containing sulfur such as PCC-DTT and PCC-BDT showed relatively lower V_{oc} value than PCC. This discrepancy was linked to the E_{LUMO} values trend, which followed the order of PCC-TAZ = PCC-TPA > PCC-CBZ > PCC-DTT > PCC-BDT dyes, as V_{oc} was derived from the E_{LUMO} value. Overall, PCC-based dyes incorporated by the donor group which was more expanded π-conjugated and containing nitrogen demonstrated better photovoltaic characteristics.

4. Conclusion

In this study, our objective was to enhance the performance of the organic compound PCC as a sensitizer for DSSCs by strategically incorporating electron donor groups identified through a comprehensive literature review. We selected various donor moieties namely, DTT, BDT, TPA, CBZ, and TAZ based on theoretical calculations using DFT and TD-DFT methods. Our structural analysis revealed that larger and more electron-rich donor groups strengthened the connection between the donor and the π-conjugated unit. Among the derivatives, PCC-BDT exhibited the most promising results, characterized by improved electronic and optical properties, including lower HOMO energy levels, a narrow energy gap (E_{gap}), enhanced absorption intensity, and a redshift in absorption peaks. Furthermore, our assessment of photovoltaic properties indicated negative electron injection free energy for all derivatives, facilitating spontaneous electron injection from the dye compounds to the TiO_2 conduction band. Notably, PCC-TAZ demonstrated the lowest ΔG_{reg}, suggesting efficient electron regeneration potential. Overall, our findings underscore the significance of molecular engineering in achieving optimal light harvesting, efficient electron injection, and enhanced power conversion efficiency in DSSCs.

CRediT authorship contribution statement

Emilia Abdulmalek: Writing – review & editing, Validation, Supervision, Software, Investigation, Funding acquisition. **Maadh Nassar:** Writing – review & editing, Writing – original draft, Visualization, Validation, Supervision, Methodology, Formal analysis. **Shahrul**

Table 3
The calculated values of electrochemical parameters for PCC and its derivatives at B3PW91/6-31G(d) level.

Dye	E_{OX}^{dye} (eV)	E_{OX}^{dye*} (eV)	E_{ex} (eV)	ΔG_{inj} (eV)	ΔG_{reg} (eV)	LHE (λ)	V_{oc} (V)
PCC	5.33	2.43	2.90	-1.57	0.53	0.9164	1.82
PCC-DTT	5.33	2.48	2.85	-1.52	0.53	0.0225	1.74
PCC-BDT	5.33	2.58	2.75	-1.42	0.53	0.0124	1.63
PCC-TPA	5.28	2.39	2.89	-1.61	0.48	0.9249	1.84
PCC-CBZ	5.33	2.41	2.92	-1.59	0.53	0.9285	1.83
PCC-TAZ	5.19	2.36	2.83	-1.64	0.39	0.9459	1.84

Ahmad: Supervision, Software, Resources, Investigation, Funding acquisition, Formal analysis. **Mohd F. Ismail:** Methodology, Investigation, Formal analysis, Data curation, Conceptualization.

Declaration of Competing Interest

The authors declare that they have no known competing financial interests or personal relationships that could have appeared to influence the work reported in this paper.

Acknowledgements

We would like to thank Malaysia Ministry of Higher Education for MFN's graduate research allowance (GRA) for funding under grant FRGS/1/2020/STG04/UPM/02/12.

Appendix A. Supporting information

Supplementary data associated with this article can be found in the online version at doi:10.1016/j.ijoes.2024.100715.

References

[1] K. Khan, A.K. Tareen, M. Iqbal, Z. Shi, H. Zhang, Z. Guo, Novel emerging graphdiyne based two dimensional materials: synthesis, properties and renewable energy applications, Nano Today 39 (2021) 101207, https://doi.org/10.1016/j.nantod.2021.101207.
[2] M. Mahar Gul, K. Shahzad Ahmad, A. Guy Thomas, A.M. Tawfeek, Advancing photoelectrochemical systems: unleashing the remarkable performance of In: SnO_2/$Nd_4In_5S_{13}$ for sustainable energy applications, ChemistrySelect 9 (2024) e202304530, https://doi.org/10.1002/slct.202304530.
[3] J.-X. Zhang, Z.-Y. Zhao, A comprehensive review on the preparation and applications of delafossite $CuAlO_2$ optoelectronic functional materials, Mater. Sci. Semicond. Process. 167 (2023) 107819, https://doi.org/10.1016/j.mssp.2023.107819.
[4] F.A. Ansari, A. Haleem, S. Bahl, M. Javaid, D. Buddhi, C. Prakash, R.C. Sharma, Advancement in solar energy technology and its future growth, in: Proceedings of the Biennial International Conference on Future Learning Aspects of Mechanical Engineering, Springer, 2022, pp. 347–57. ⟨https://doi.org/10.1007/978-981-99-2382-3_29⟩.
[5] A. Boutramine, S. Al-Qaisi, S. Samah, N. Iram, T.A. Alrebdi, S. Bouzgarrou, A. S. Verma, S. Belhachi, R. Sharma, Optoelectronic and thermoelectric properties of new lead-free K_2NaSbZ_6 (Z = Br, I) halide double-perovskites for clean energy applications: a DFT study, Opt. Quantum Electron. 56 (2024) 417, https://doi.org/10.1007/s11082-024-06344-4.
[6] J. Vetrovec, A.S. Litt, D.A. Copeland, J. Junghans, R. Durkee, Liquid metal heat sink for high-power laser diodes, in: High-Power Diode Laser Technology and Applications XI, SPIE, 2013, pp. 95–101, https://doi.org/10.1117/12.2005357.
[7] R.P. Stumpf, T.W. Davis, T.T. Wynne, J.L. Graham, K.A. Loftin, T.H. Johengen, D. Gossiaux, D. Palladino, A. Burtner, Challenges for mapping cyanotoxin patterns from remote sensing of cyanobacteria, Harmful Algae 54 (2016) 160–173, https://doi.org/10.1016/j.hal.2016.01.005.
[8] J. Li, Q. Bao, C.M. Li, W. Zhang, C. Gong, M.B. Chan-Park, J. Qin, B.S. Ong, Organic thin-film transistors processed from relatively nontoxic, environmentally friendlier solvents, Chem. Mater. 22 (2010) 5747–5753, https://doi.org/10.1021/cm102071m.
[9] A. Gupta, S. Sharma, R. Gupta, A. Sharma, M. Tomar, Exploitation of electric field assisted optical signal amplification in ferroelectric photorefractive $K_{0.50}Na_{0.50}NbO_3$ thin film, Opt. Mater. 121 (2021) 111599, https://doi.org/10.1016/j.optmat.2021.111599.
[10] S.M. Jain, T. Edvinsson, J.R. Durrant, Green fabrication of stable lead-free bismuth based perovskite solar cells using a non-toxic solvent, Commun. Chem. 2 (2019) 91, https://doi.org/10.1038/s42004-019-0195-3.
[11] A. Sen, M.H. Putra, A.K. Biswas, A.K. Behera, A. Groβ, Insight on the choice of sensitizers/dyes for dye sensitized solar cells: a review, Dyes Pigments (2023) 111087, https://doi.org/10.1016/j.dyepig.2023.111087.
[12] N. Tomar, A. Agrawal, V.S. Dhaka, P.K. Surolia, Ruthenium complexes based dye sensitized solar cells: fundamentals and research trends, Sol. Energy 207 (2020) 59–76, https://doi.org/10.1016/j.solener.2020.06.060.
[13] A. Mani, T. Feng, A. Gandioso, R. Vinck, A. Notaro, L. Gourdon, P. Burckel, B. Saubaméa, O. Blacque, K. Cariou, Structurally simple osmium (II) polypyridyl complexes as photosensitizers for photodynamic therapy in the near infrared, Angew. Chem. 135 (2023) e202218347, https://doi.org/10.1002/ange.202218347.
[14] V. Hegde, N.V. Kulkarni, Sustainable late transition metal-based dyes for dye-sensitized solar cells, Comments Inorg. Chem. (2024) 1–79, https://doi.org/10.1080/02603594.2024.2309881.
[15] F.-S. Lin, P. Priyanka, M.-S. Fan, S. Vegiraju, J.-S. Ni, Y.-C. Wu, Y.-H. Li, G.-H. Lee, Y. Ezhumalai, R.-J. Jeng, Metal-free efficient dye-sensitized solar cells based on thioalkylated bithiophenyl organic dyes, J. Mater. Chem. C Mater. 8 (2020) 15322–15330, https://doi.org/10.1039/D0TC02310H.
[16] P. Ferdowsi, Y. Saygili, F. Jazaeri, T. Edvinsson, J. Mokhtari, S.M. Zakeeruddin, Y. Liu, M. Grätzel, A. Hagfeldt, Molecular engineering of simple metal-free organic dyes derived from triphenylamine for dye-sensitized solar cell applications, ChemSusChem 13 (2020) 212–220, https://doi.org/10.1002/cssc.201902245.
[17] A. Dessì, D.A. Chalkias, S. Bilancia, A. Sinicropi, M. Calamante, A. Mordini, A. Karavioti, E. Stathatos, L. Zani, G. Reginato, D–A–π–A organic dyes with tailored green light absorption for potential application in greenhouse-integrated dye-sensitized solar cells, Sustain Energy Fuels 5 (2021) 1171–1183, https://doi.org/10.1039/D0SE01610A.
[18] S. Rahman, A. Haleem, M. Siddiq, M.K. Hussain, S. Qamar, S. Hameed, M. Waris, Research on dye sensitized solar cells: recent advancement toward the various constituents of dye sensitized solar cells for efficiency enhancement and future prospects, RSC Adv. 13 (2023) 19508–19529, https://doi.org/10.1039/D3RA00903C.
[19] Ekhlas Abd-Alkuder Salman, Maadh Fawzi Nassar Khalida Abaid Samawi, G. Abdulkareem-Alsultan, Emilia Abdulmalek, 3D hollow spheres comprising MXene/g-C3N4 heterostructre for efficient polysulfide adsorption and conversion in high-performance Li-S batteries, J. Electroanal. Chem. 945 (2023) 117629, https://doi.org/10.1016/j.jelechem.2023.117629.
[20] J.-M. Ji, H. Zhou, H.K. Kim, Rational design criteria for D–π–A structured organic and porphyrin sensitizers for highly efficient dye-sensitized solar cells, J. Mater. Chem. A Mater. 6 (2018) 14518–14545, https://doi.org/10.1039/C8TA02281J.
[21] H.J. Noh, J.-M. Ji, S.P. Hwang, C.H. Kim, H.K. Kim, D-π-A-structured organic sensitizers with π-extended auxiliary acceptor units for high-performance dye-sensitized solar cells, Dyes Pigments 195 (2021) 109681, https://doi.org/10.1016/j.dyepig.2021.109681.
[22] Nassar, F. Maadh, Emilia Abdulmalek, Mohd F. Ismail, Shahrul Ainliah Alang Ahmad, G. Abdulkreem-Alsultan, Recent progress in benzimidazole and quinoxaline dyes based on dye-sensitized solar cells: a comprehensive overview, High Energy Chem. 58 (1) (2024) 16–58, https://doi.org/10.1134/S0018143924010132.
[23] R. Grisorio, L. De Marco, R. Agosta, R. Iacobellis, R. Giannuzzi, M. Manca, P. Mastrorilli, G. Gigli, G.P. Suranna, Enhancing dye-sensitized solar cell performances by molecular engineering: highly efficient π-extended organic sensitizers, ChemSusChem 7 (2014) 2659–2669, https://doi.org/10.1002/cssc.201402164.
[24] F. Arkan, F. Pakravesh, F. Barati Darband, S. Sabagh, M. Izadyar, Recent progress toward high-performance dye-sensitized solar cells: a review, J. Iran. Chem. Soc. (2024) 1–62, https://doi.org/10.1007/s13738-024-02967-2.
[25] H.-Y. Yang, Y.-S. Yen, Y.-C. Hsu, H.-H. Chou, J.T. Lin, Organic dyes incorporating the dithieno [3, 2-*b*: 2′, 3′-*d*] thiophene moiety for efficient dye-sensitized solar cells, Org. Lett. 12 (2010) 16–19, https://doi.org/10.1021/ol902327p.
[26] J. Xu, J. Zhang, D. Yang, K. Yu, D. Li, Z. Xia, Z. Ge, Two star-shaped small molecule donors based on benzodithiophene unit for organic solar cells, Chin. Chem. Lett. 33 (2022) 247–251, https://doi.org/10.1016/j.cclet.2021.06.023.
[27] J. He, Y. Liu, J. Gao, L. Han, New D—D—π-A triphenylamine–coumarin sensitizers for dye-sensitized solar cells, Photochem. Photobiol. Sci. 16 (2017) 1049–1056, https://doi.org/10.1039/c6pp00410e.
[28] Z. Wan, C. Jia, Y. Wang, J. Luo, X. Yao, Significant improvement of phenothiazine organic dye-sensitized solar cell performance using dithiafulvenyl unit as additional donor, Org. Electron. 27 (2015) 107–113, https://doi.org/10.1016/j.orgel.2015.09.009.

[29] K. Srinivas, C.R. Kumar, M.A. Reddy, K. Bhanuprakash, V.J. Rao, L. Giribabu, D-π-A organic dyes with carbazole as donor for dye-sensitized solar cells, Synth. Met. 161 (2011) 96–105, https://doi.org/10.1016/j.synthmet.2010.11.004.
[30] X. Qian, L. Lu, Y.-Z. Zhu, H.-H. Gao, J.-Y. Zheng, Triazatruxene-based organic dyes containing a rhodanine-3-acetic acid acceptor for dye-sensitized solar cells, Dyes Pigments 113 (2015) 737–742, https://doi.org/10.1016/j.dyepig.2014.10.007.
[31] N. Sudha, R. Surendran, S. Jeyaram, Synthesis, characterization, linear and nonlinear optical features of novel organic compound pyridylcarboxamide chalcone for nonlinear optical applications, Opt. Mater. 131 (2022) 112668, https://doi.org/10.1016/j.optmat.2022.112668.
[32] Atef El Jery, Hayder Mahmood Salman, Rusul Mohammed Al-Khafaji, Maadh Fawzi Nassar, Mika Sillanpää, Thermodynamics Investigation and artificial neural network prediction of energy, exergy, and hydrogen production from a solar thermochemical plant using a polymer membrane electrolyzer, Molecules 28 (6) (2023) 2649, https://doi.org/10.3390/molecules28062649.
[33] M. Frisch, G.W. Trucks, H.B. Schlegel, G.E. Scuseria, M.A. Robb, J.R. Cheeseman, G. Scalmani, V. Barone, B. Mennucci, Ga Petersson, Gaussian 09. Revision d. 01, Gaussian, Inc., Wallingford CT, 2009, p. 201.
[34] G. Deogratias, N. Seriani, T. Pogrebnaya, A. Pogrebnoi, Tuning optoelectronic properties of triphenylamine based dyes through variation of pi-conjugated units and anchoring groups: a DFT/TD-DFT investigation, J. Mol. Graph. Model. 94 (2020) 107480, https://doi.org/10.1016/j.jmgm.2019.107480.
[35] E. Cances, B. Mennucci, J. Tomasi, A new integral equation formalism for the polarizable continuum model: theoretical background and applications to isotropic and anisotropic dielectrics, J. Chem. Phys. 107 (1997) 3032–3041, https://doi.org/10.1063/1.474659.
[36] D. Fadili, Z.M.E. Fahim, S.M. Bouzzine, O.T. Alaoui, M. Hamidi, Effects of auxiliary electron-withdrawing moieties on the photovoltaic properties of D-π-A'-π-A phosphonic acid-based DSSCs, Comput. Theor. Chem. 1210 (2022) 113645, https://doi.org/10.1016/j.comptc.2022.113645.
[37] M. Yousefzadeh Borzehandani, E. Abdulmalek, M.B. Abdul Rahman, M. A. Mohammad Latif, First-principles investigation of dimethyl-functionalized MIL-53 (Al) metal–organic framework for adsorption and separation of xylene isomers, J. Porous Mater. 28 (2021) 579–591, https://doi.org/10.1007/s10934-020-01016-6.
[38] Y. Boughoues, M. Benamira, L. Messaadia, N. Ribouh, Adsorption and corrosion inhibition performance of some environmental friendly organic inhibitors for mild steel in HCl solution via experimental and theoretical study, Colloids Surf. A Physicochem Eng. Asp. 593 (2020) 124610, https://doi.org/10.1016/j.colsurfa.2020.124610.
[39] Y. Boughoues, M. Benamira, L. Messaadia, N. Bouider, S. Abdelaziz, Experimental and theoretical investigations of four amine derivatives as effective corrosion inhibitors for mild steel in HCl medium, RSC Adv. 10 (2020) 24145–24158, https://doi.org/10.1039/D0RA03560B.
[40] M. Lazrak, H. Toufik, S.M. Bouzzine, F. Lamchouri, Bridge effect on the charge transfer and optoelectronic properties of triphenylamine-based organic dye sensitized solar cells: theoretical approach, Res. Chem. Intermed. 46 (2020) 3961–3978, https://doi.org/10.1007/s11164-020-04184-x.
[41] M.-W. Lee, J.-Y. Kim, H.-G. Lee, H.G. Cha, D.-H. Lee, M.J. Ko, Effects of structure and electronic properties of D-π-A organic dyes on photovoltaic performance of dye-sensitized solar cells, J. Energy Chem. 54 (2021) 208–216, https://doi.org/10.1016/j.jechem.2020.05.060.
[42] I.M. Abdellah, M.R. Eletmany, A. El-Shafei, Exploring the impact of electron acceptor tuning in D-π-A′-π-A photosensitizers on the photovoltaic performance of acridine-based DSSCs: a DFT/TDDFT perspective, Mater. Today Commun. 35 (2023) 106170, https://doi.org/10.1016/j.mtcomm.2023.106170.
[43] B. Dulo, K. Phan, J. Githaiga, K. Raes, S. De Meester, Natural quinone dyes: a review on structure, extraction techniques, analysis and application potential, Waste Biomass Valoriz. 12 (2021) 6339–6374, https://doi.org/10.1007/s12649-021-01443-9.
[44] F. Luan, X. Xu, H. Liu, M.N.D.S. Cordeiro, Review of quantitative structure-activity/property relationship studies of dyes: recent advances and perspectives, Color. Technol. 129 (2013) 173–186, https://doi.org/10.1111/cote.12027.
[45] Harismah, Kun, Maadh Fawzi Nassar, Omar Talal Hamid, Mohsin O. AL-Khafaji, Hasan Zandi. Investigating a Boron Nitride Plate for the Formaldehyde Adsorption: Density Functional Theory Calculations, vol. 13, 2022, 346. ⟨https://doi.org/10.33263/BRIAC134.346⟩.
[46] K. Periyasamy, P. Sakthivel, G. Venkatesh, P. Vennila, Y. Sheena Mary, Synthesis and design of carbazole-based organic sensitizers for DSSCs applications: experimental and theoretical approaches, Chem. Pap. 78 (2024) 447–461, https://doi.org/10.1007/s11696-023-03101-x.
[47] K.A. Samawi, E.A.A. Salman, B.A.A. Alshekhly, M.F. Nassar, M.Y. Borzehandani, G. Abdulkareem-Alsultan, M.A.M. Latif, E. Abdulmalek, Rational design of different π-bridges and their theoretical impact on indolo [3, 2, 1-*jk*] carbazole based dye-sensitized solar cells, Comput. Theor. Chem. 1212 (2022) 113725, https://doi.org/10.1016/j.comptc.2022.113725.
[48] F.C. Asogwa, H. Louis, U.S. Ameuru, T.O. Unimuke, K.A. Adegoke, T.O. Magu, E. C. Agwamba, Experimental and theoretical studies of the influence of alkyl groups on the photovoltaic properties of (*E*)-6-((2, 3-dihydroxylnaphthalene) diazenyl)-1H-benzoisoquinoline-1, 3-dione-based organic solar cell, J. Mol. Model. 28 (2022) 245, https://doi.org/10.1007/s00894-022-05228-2.
[49] M.M. Makhlouf, A.S. Radwan, B. Ghazal, Experimental and DFT insights into molecular structure and optical properties of new chalcones as promising photosensitizers towards solar cell applications, Appl. Surf. Sci. 452 (2018) 337–351, https://doi.org/10.1016/j.apsusc.2018.05.007.
[50] S. TamilSelvan, A. Prakasam, G. Venkatesh, C. Kamal, Y. Sheena Mary, S. Parveen Banu, P. Vennila, Y. Shyma Mary, Synthesis, spectral characterizations, molecular geometries and electronic properties of phenothiazine based organic dyes for dye-sensitized solar cells, Z. für Phys. Chem. 235 (2021) 1355–1380, https://doi.org/10.1515/zpch-2020-1732.
[51] T.S. Kumaran, A. Prakasam, P.M. Anbarasan, P. Vennila, G. Venkatesh, S.P. Banu, Y.S. Mary, New phenoxazine-based organic dyes with various acceptors for dye-sensitized solar cells: synthesis, characterization, DSSCs fabrications and DFT study, J. Comput. Biophys. Chem. 20 (2021) 465–476, https://doi.org/10.1142/S2737416521500253.
[52] T.S. Kumaran, A. Prakasam, P.M. Anbarasan, P. Vennila, G. Venkatesh, S.P. Banu, Y.S. Mary, New phenoxazine-based organic dyes with various acceptors for dye-sensitized solar cells: synthesis, characterization, DSSCs fabrications and DFT study, J. Comput. Biophys. Chem. 20 (2021) 465–476, https://doi.org/10.1142/S2737416521500253.
[53] K. Periyasamy, P. Sakthivel, G. Venkatesh, P.M. Anbarasan, P. Vennila, Y. Sheena Mary, S. Kaya, S. Erkan, Synthesis, photophysical, electrochemical, and DFT examinations of two new organic dye molecules based on phenothiazine and dibenzofuran, J. Mol. Model. 28 (2022) 34, https://doi.org/10.1007/s00894-022-05026-w.
[54] K. Periyasamy, P. Sakthivel, P. Vennila, P.M. Anbarasan, G. Venkatesh, Y.S. Mary, Novel D-π-A phenothiazine and dibenzofuran organic dyes with simple structures for efficient dye-sensitized solar cells, J. Photochem. Photobiol. A Chem. 413 (2021) 113269, https://doi.org/10.1016/j.jphotochem.2021.113269.
[55] A.K. Narsaria, J. Poater, C. Fonseca Guerra, A.W. Ehlers, K. Lammertsma, F. M. Bickelhaupt, Rational design of near-infrared absorbing organic dyes: controlling the HOMO–LUMO gap using quantitative molecular orbital theory, J. Comput. Chem. 39 (2018) 2690–2696, https://doi.org/10.1002/jcc.25731.
[56] S. Shahab, M. Sheikhi, L. Filippovich, M. Khaleghian, E. Dikusar, H. Yahyaei, M. Y. Borzehandani, Spectroscopic studies (geometry optimization, E→ Z isomerization, UV/Vis, excited states, FT-IR, HOMO-LUMO, FMO, MEP, NBO, Polarization) and anisotropy of thermal and electrical conductivity of new azomethine dyes in stretched polymer matrix, Silicon 10 (2018) 2361–2385, https://doi.org/10.1007/s12633-018-9773-8.
[57] H. Yahyaei, S. Shahab, M. Sheikhi, L. Filippovich, H.A. Almodarresiyeh, R. Kumar, E. Dikusar, M.Y. Borzehandani, R. Alnajjar, Anisotropy (optical, electrical and thermal conductivity) in thin polarizing films for UV/Vis regions of spectrum: experimental and theoretical investigations, Spectrochim. Acta A Mol. Biomol. Spectrosc. 192 (2018) 343–360, https://doi.org/10.1016/j.saa.2017.11.029.
[58] B. Kim, X. Ma, C. Chen, Y. Ie, E.W. Coir, H. Hashemi, Y. Aso, P.F. Green, J. Kieffer, J. Kim, Energy level modulation of HOMO, LUMO, and band-gap in conjugated polymers for organic photovoltaic applications, Adv. Funct. Mater. 23 (2013) 439–445, https://doi.org/10.1002/adfm.201201385.
[59] Z. Zheng, N.R. Tummala, Y.-T. Fu, V. Coropceanu, J.-L. Brédas, Charge-transfer states in organic solar cells: understanding the impact of polarization, delocalization, and disorder, ACS Appl. Mater. Interfaces 9 (2017) 18095–18102, https://doi.org/10.1021/acsami.7b02193.
[60] M.I. Nabeel, D. Hussain, N. Ahmad, H.-M. Xiao, S.G. Musharraf, Improved visible light-driven photocatalytic degradation of an industrial dye Acid Orange 7 using metal-free sulfur-doped graphitic carbon nitride, Environ. Sci. Nano 10 (2023) 2810–2830, https://doi.org/10.1039/D3EN00289F.
[61] F. Lin, Y. Zhang, L. Wang, Y. Zhang, D. Wang, M. Yang, J. Yang, B. Zhang, Z. Jiang, C. Li, Highly efficient photocatalytic oxidation of sulfur-containing organic compounds and dyes on TiO_2 with dual cocatalysts Pt and RuO_2, Appl. Catal. B 127 (2012) 363–370, https://doi.org/10.1016/j.apcatb.2012.08.024.
[62] N. Arslan, N. Yildirir, A.M. Sevim, S. Çakar, M. Özacar, A. Gül, Sulfur-bridged oxotitanium phthalocyanine-and porphyrin-based cocktail dyes as sensitizers for improved dye sensitized solar cell efficiency, Dyes Pigments 220 (2023) 111623, https://doi.org/10.1016/j.dyepig.2023.111623.
[63] E. Hosseinzadeh, N.L. Hadipour, G. Parsafar, A computational investigation on the influence of different π spacer groups in the bithiazole-based organic dye sensitizers on the short-circuit photocurrent densities of dye-sensitized solar cells, J. Photochem. Photobiol. A Chem. 333 (2017) 70–78, https://doi.org/10.1016/j.jphotochem.2016.10.010.
[64] M.U. Khan, M. Khalid, M. Ibrahim, A.A.C. Braga, M. Safdar, A.A. Al-Saadi, M.R.S. A. Janjua, First theoretical framework of triphenylamine–dicyanovinylene-based nonlinear optical dyes: structural modification of π-linkers, J. Phys. Chem. C 122 (2018) 4009–4018, https://doi.org/10.1021/acs.jpcc.7b12293.
[65] I. Zubair, R.A. Kher, S.J. Akram, Y.A. El-Badry, M.U. Saeed, J. Iqbal, Tuning the optoelectronic properties of indacenodithiophene based derivatives for efficient photovoltaic applications: a DFT approach, Chem. Phys. Lett. 793 (2022) 139459, https://doi.org/10.1016/j.cplett.2022.139459.
[66] J. Zhang, H.-B. Li, S.-L. Sun, Y. Geng, Y. Wu, Z.-M. Su, Density functional theory characterization and design of high-performance diarylamine-fluorene dyes with different π spacers for dye-sensitized solar cells, J. Mater. Chem. 22 (2012) 568–576, https://doi.org/10.1039/C1JM13028E.
[67] N.A. Wazzan, A DFT/TDDFT investigation on the efficiency of novel dyes with ortho-fluorophenyl units (A1) and incorporating benzotriazole/benzothiadiazole/phthalimide units (A2) as organic photosensitizers with D–A2–π–A1 configuration for solar cell applications, J. Comput. Electron. 18 (2019) 375–395, https://doi.org/10.1007/s10825-019-01308-4.
[68] L.L. Estrella, M.P. Balanay, D.H. Kim, The effect of donor group rigidification on the electronic and optical properties of arylamine-based metal-free dyes for dye-sensitized solar cells: a computational study, J. Phys. Chem. A 120 (2016) 5917–5927, https://doi.org/10.1021/acs.jpca.6b03271.

[69] R. Dutta, S. Ahmed, D.J. Kalita, Theoretical design of new triphenylamine based dyes for the fabrication of DSSCs: a DFT/TD-DFT study, Mater. Today Commun. 22 (2020) 100731, https://doi.org/10.1016/j.mtcomm.2019.100731.
[70] M.I. Khan, J. Iqbal, S.J. Akram, Y.A. El-Badry, M. Yaseen, R.A. Khera, End-capped group modification on cyclopentadithiophene based non-fullerene small molecule acceptors for efficient organic solar cells; a DFT approach, J. Mol. Graph. Model. 113 (2022) 108162, https://doi.org/10.1016/j.jmgm.2022.108162.
[71] E. Cances, B. Mennucci, J. Tomasi, A new integral equation formalism for the polarizable continuum model: theoretical background and applications to isotropic and anisotropic dielectrics, J. Chem. Phys. 107 (1997) 3032–3041, https://doi.org/10.1063/1.474659.